Inorg. Chem. **1995,** *34,* 49−54

Synthesis and Characterization of the New Selenolate Ligand $-SeC_6H_3$-2,6-Mes_2 (Mes = C_6H_2-2,4,6-Me_3) and Its Two-Coordinate Zinc and Manganese Derivatives: Factors Affecting Bending in Two-Coordinate Metal Complexes with Aryl-Substituted Ligands

Jeffrey J. Ellison, Karin Ruhlandt-Senge, Håkon H. Hope, and Philip P. Power*

Department of Chemistry, University of California, Davis, California 95616

Received August 24, 1994[⊛]

The synthesis and characterization of a novel sterically demanding selenol $HSeC_6H_3$-2,6-Mes_2, **1** (Mes = $-C_6H_2$-2,4,6-Me_3), the corresponding diselenide, **2**, and some of its metal derivatives are described. Solvated and unsolvated zinc selenolates were prepared by the treatment of the amide $Zn\{N(SiMe_3)_2\}_2$ in hexane with 2 equiv of the bulky selenol, **1**. Crystallization from hexane produces monomeric $Zn(SeC_6H_3$-2,6-$Mes_2)_2$, **3**, while crystallization from tetrahydrofuran results in the monomeric adduct $Zn(SeC_6H_3$-2,6-$Mes_2)_2$(THF), **4**. Treatment of $Mn\{N(SiMe_3)_2\}_2$ with 2 equiv of **1** and crystallization from methylene chloride yields $Mn(SeC_6H_3$-2,6-$Mes_2)_2{\cdot}2CH_2Cl_2$, **5**$\cdot 2CH_2Cl_2$. The synthesis and structure determination of $[Mn(SeMes^*)_2THF]_2{\cdot}4PhMe$ (Mes* = $-C_6H_2$-2,4,6-t-Bu_3), **6**, were also undertaken to compare the steric properties of the $-SeC_6H_3$-2,6-Mes_2 and $-SeMes^*$ ligands. The compounds **1**−**5** were characterized by IR and ^1H NMR spectroscopy, and **1**−**4** were also characterized by ^{77}Se NMR spectroscopy. The structures of **2**−**6** were determined by X-ray crystallography. In **3** the zinc has a crystallographically required linear coordination whereas the manganese atom in **5** has a bent geometry with a Se−Mn−Se angle of 119.9(1)°. In contrast, the structure of **6** is dimeric even in the presence of THF donor ligands. Crystal data with Mo Kα (λ = 0.710 69 Å) (**2** and **5**) or Cu Kα (λ = 1.541 78 Å) (**3** and **4**) radiation at 130 K: **2**, a = 16.144(4) Å, b = 15.122(3) Å, c = 16.155(4) Å, β = 91.86(2)°, monoclinic, Z = 4, space group $P2_1/n$, R = 0.056; **3**, a = 9.318(2) Å, b = 10.904(4) Å, c = 11.796(4) Å, α = 62.25(2)°, β = 73.76(2)°, γ = 68.92(2)°, triclinic, Z = 2, space group $P\bar{1}$, R = 0.059; **4**, a = 10.621(3) Å, b = 10.828(3) Å, c = 22.491(6) Å, α = 86.76(2)°, β = 85.20(2)°, γ = 60.57(2)°, triclinic, Z = 2, space group $P\bar{1}$, R = 0.073; **5**$\cdot 2CH_2Cl_2$, a = 20.061(5) Å, b = 14.705(5) Å, c = 15.781(5) Å, orthorhombic, Z = 8, space group $Pccn$, R = 0.063; **6**$\cdot$4PhMe, a = 19.000(8) Å, b = 19.626(6) Å, c = 27.687(7) Å, β = 98.18(5)°, Z = 4, space group $P2_1/n$, R = 0.086.

Introduction

Interest in metal selenolate complexes stems from their potential use as precursors for M/Se materials[1−3] and their relevance as models for the active sites of selenocysteine-containing metalloproteins.[4−7] In spite of the large number of metal selenolates known and the general interest in metal selenolate complexes, the number of structural types are, with few a exceptions, limited to anionic[5,8−10] and mixed-ligand species[6,7,11−15] with the metal in a coordination number of 4. Apart from the dimeric species $[Cd(SeMes^*)_2]_2$[2] (Mes* = C_6H_2-2,4,6-t-Bu_3) and $[Pb\{SeC_6H_2$-2,4,6-$(CF_3)_3\}_2]_2$[15] and the monomeric $M(SeMes^*)_3$ (M = Ga, In),[16] structurally characterized neutral molecular homoleptic metal selenolates have not been reported. This is a consequence of the strong tendency of metal selenolates to form noncrystalline insoluble polymers through bridging by the chalcogenolate ligands.[17] It has been shown in the case of thiolate complexes that extensive association through sulfur bridging can often be avoided through the use of sterically demanding thiolates, the most common of which uses the $-$Mes* group to provide steric hindrance. Examples of such complexes are $Sn(SMes^*)_2$ and $[M(SMes^*)_2]_2$ (M = Mn,[18] Fe,[18] Co,[18] Zn[19]). Extensive studies on metal tellurolates have also been published, and neutral homoleptic tellurolates of the formula $[M\{TeSi(SiMe_3)_3\}_2]$ (M = Zn,[20a] Cd,[20a] Hg,[20a] Sn,[20b] Au,[20c] Ag[20d]) have been reported.[20] Metal derivatives of the selenolate ligand $-$SeMes* are not as well studied, but there is

---

[⊛] Abstract published in *Advance ACS Abstracts,* December 1, 1994.

(1) (a) Brennan, J. G.; Siegrist, T.; Carroll, P. J.; Stuczynski, S. M.; Brus, L. E.; Steigerwald, M. L. *J. Am. Chem. Soc.* **1989**, *111*, 4141. (b) Brennan, J. G.; Siegrist, T.; Carroll, P. J.; Stuczynski, S. M.; Reynders, P.; Brus, L. E.; Steigerwald, M. L. *Chem. Mater.* **1990**, *2*, 403.

(2) Bochmann, M.; Webb, K. J.; Hursthouse, M. B.; Mazid, M. *J. Chem. Soc., Dalton Trans.* **1991**, 2317. Bochmann, M.; Webb, K.; Harman, M.; Hursthouse, M. B. *Angew. Chem.* **1990**, *102*, 703; *Angew. Chem., Int. Ed. Engl.* **1990**, *29*, 638.

(3) Kanatzidis, M. G.; Huang, S. *Coord. Chem. Rev.* **1994**, *130*, 509.

(4) (a) Stadtman, T. C. *Annu. Rev. Biochem.* **1990**, *59*, 11. (b) Yu, S.-B.; Papaefthymiou, G. C.; Holm, R. H. *Inorg. Chem.* **1991**, *30*, 3476.

(5) Ueyama, N.; Sugawara, T.; Sasaki, K.; Nakamura, A.; Yamashita, S.; Wakatsuki, Y.; Yamazaki, H.; Yasuoka, N. *Inorg. Chem.* **1988**, *27*, 741.

(6) Bochmann, M.; Webb, K. J.; Hursthouse, M. B.; Mazid, M. *J. Chem. Soc., Chem. Commun.* **1991**, 1735.

(7) Baidya, N.; Noll, B. C.; Olmstead, M. M.; Mascharak, P. K. *Inorg. Chem.* **1992**, *31*, 2999.

(8) McConnachie, J. M.; Ibers, J. A. *Inorg. Chem.* **1991**, *30*, 1770.

(9) Tremel, W.; Krebs, B.; Griewe, K.; Simon, W.; Stephen, H.-O.; Henkel, G. *Z. Naturforsch., B.* **1992**, *47*, 1580.

(10) Vittal, J. J.; Dean, P. A. W.; Payne, N. C. *Can. J. Chem.* **1992**, *70*, 792.

(11) Bochmann, M.; Coleman, A. P.; Powell, A. K. *Polyhedron* **1992**, *11*, 507.

(12) Bochmann, M.; Bwembya, G. C.; Powell, A. K. *Polyhedron* **1993**, *12*, 2929.

(13) Bochmann, M.; Powell, A. K.; Song, X. *Inorg. Chem.* **1994**, *33*, 400.

(14) Bochmann, M.; Bwembya, G. C.; Grinter, R.; Powell, A. K.; Webb, K. J.; Hursthouse, M. B.; Malik, K. M. A.; Mazid, M. A. *Inorg. Chem.* **1994**, *33*, 2290.

(15) Labahn, D.; Bohnen, F. M.; Herbst-Irmer, R.; Pohl, E.; Stalke, D.; Roesky, H. W. *Z. Anorg. Allg. Chem.* **1994**, *620*, 41.

(16) Ruhlandt-Senge, K.; Power, P. P. *Inorg. Chem.* **1991**, *30*, 3683; **1993**, *32*, 3478.

(17) Dance, I. G. *Polyhedron* **1986**, *5*, 1037. Blower, P. J.; Dilworth, J. R. *Coord. Chem. Rev.* **1987**, *76*, 121.

(18) Power, P. P.; Shoner, S. C. *Angew. Chem., Int. Ed. Engl.* **1991**, *30*, 330.

0020-1669/95/1334-0049$09.00/0

some evidence that they may display an even stronger tendency to associate than the corresponding thiolates. Thus a dimeric structure was observed in the case of $[Zn(SeMes^*)_2(p\text{-}O{=}CHC_6H_4OMe)]_2$,[6] whereas unassociated structures were observed in a number of related thiolate derivatives of a similar formula $Zn(SMes^*)_2L$ ($L = Et_2O$,[19a] pyridine,[14] tetrahydrothiophene,[14] phosphine[14]). In addition, a dimeric structure has been observed for $[Mn\{N(SiMe_3)_2\}(\mu\text{-}SeC_6H_2\text{-}2,4,6\text{-}i\text{-}Pr_3)(THF)]_2$[13] even in the presence of THF donor molecules. Recent work showed that the use of the more sterically demanding aryl substituent $-C_6H_3$-2,6-Mes_2 (Mes = C_6H_2-2,4,6-Me_3) at sulfur enables the isolation of the monomeric two-coordinate metal thiolates $M(SC_6H_3\text{-}2,6\text{-}Mes_2)_2$ (M = Fe,[21] Zn[22]). In this paper it is shown that the $-C_6H_3$-2,6-Mes_2 group is also effective in stabilizing unassociated two-coordinate metal selenolates. Specifically, the syntheses and characterizations of a novel bulky selenol $HSeC_6H_3$-2,6-Mes_2, **1**, diselenide $[SeC_6H_3\text{-}2,6\text{-}Mes_2]_2$, **2**, zinc derivatives $Zn(SeC_6H_3\text{-}2,6\text{-}Mes_2)_2$, **3**, and $Zn(SeC_6H_3\text{-}2,6\text{-}Mes_2)_2(THF)$, **4**, and the manganese derivative $Mn(SeC_6H_3\text{-}2,6\text{-}Mes_2)_2$, **5**, are described. In addition, the synthesis and structure of the associated species $[Mn(SeMes^*)_2(THF)]_2{\cdot}4PhMe$, **6**, are reported. Compounds **3** and **5** represent the first structurally characterized examples of homoleptic two-coordinate metal selenolates.

Experimental Section

General Procedures. All reactions were performed under N_2 by using either modified Schlenk techniques or a Vacuum Atmospheres HE 43-2 drybox. Solvents were freshly distilled from sodium–potassium alloy and degassed twice before use. IC_6H_3-2,6-Mes_2,[23] $Zn\{N(SiMe_3)_2\}_2$,[24] and $Mn\{N(SiMe_3)_2\}_2$[25] were prepared by published procedures. *n*-Butyllithium 1.6 M in hexanes and HBF_4 were purchased from commercial suppliers and used as received. Infrared spectra were recorded in the range 4000–200 cm^{-1} as Nujol mulls between CsI plates by using a Perkin-Elmer PE-1430 spectrometer. ^1H and ^{77}Se NMR spectra were obtained on a General Electric QE-300 spectrometer. Magnetic measurements were obtained with a Johnson-Mathey magnetic balance.

$HSeC_6H_3$-2,6-Mes_2 (1). IC_6H_3-2,6-Mes_2 (4.4 g, 10 mmol) was dissolved in hexane (50 mL), and 10 mmol of *n*-BuLi (6.25 mL of a 1.6 M solution in hexanes) was added via syringe. The solution was stirred at ambient temperature for 12 h. All volatile materials were removed under reduced pressure. The remaining solid was redissolved in THF with cooling in a dry ice bath; then 1 equiv of selenium (0.79 g, 10 mmol) was added via a solids-addition funnel. Stirring was continued for 2 h, and the reaction mixture was allowed to warm to room temperature. The volatile materials were removed under reduced pressure, and the contents of the flask were dissolved in toluene. HBF_4 (54% in diethyl ether, 8.0 mL) was added dropwise via syringe, and the resultant yellow solution was stirred for a further 2 h. The contents of the flask were allowed to settle, and the supernatant liquid was decanted via cannula into another flask. The volume was reduced to incipient crystallization and the mixture was cooled in a −20 °C freezer to produce yellow crystals of **1** in *ca.* 60% yield; mp 222–225 °C. ^1H NMR (PhMe-d_8): δ 1.14 (s, 1H, SeH), 2.08 (s, 12H, o-Me), 2.17 (s, 6H, p-Me), 6.82 (s, 4H, m-H (Mes)), 6.84 (d, 2H, m-H (Ph)), 7.04 (t, 1H, p-H). ^{77}Se NMR (PhMe-d_8): δ 66.7 (d, SeH, J = 61 Hz). IR (Nujol, ν in cm^{-1}): 2298 m (ν(Se–H)), 1715 m, 1610 s, 1565 m, 1195 w, 1030 s, 965 w, 860 s, 850 s, 810 m, 795 s, 740 s, 720 s, 580 m, 567 m, 540 m, 420 m, 335 m, 280 w.

$(SeC_6H_3\text{-}2,6\text{-}Mes_2)_2$ (2). $LiSeC_6H_3$-2,6-Mes_2 was prepared in situ in THF as described above. An aqueous basic solution of $K_3Fe(CN)_6$ was then added dropwise to effect the oxidation of the selenolate to the diselenide. The organic layer was separated and the aqueous phase extracted with diethyl ether (3 × 70 mL). The combined organic phases were dried over K_2CO_3 and filtered, and the filtrate was evaporated to dryness. Recrystallization of the residue from toluene gave deep red crystals of **2** in *ca.* 35% yield; mp 265–267 °C. ^1H NMR ($CDCl_3$): δ 1.74 (s, 12H, o-Me), 2.34 (s, 6H, p-Me), 6.75 (s, 4H, m-H (Mes)), 6.84 (d, 2H, m-H (Ph)), 7.20 (t, 1H, p-H). ^{77}Se NMR ($CDCl_3$): δ 421.5 (s). IR (Nujol, ν in cm^{-1}): 1730 w, 1610 s, 1560 w, 1300 w, 1260 w, 1175 m, 1165 w, 1155 w, 1025 m, 860 m, 845 s, 800 s, 775 m, 740 s, 720 m, 575 m.

$Zn(SeC_6H_3\text{-}2,6\text{-}Mes_2)_2$ (3). The selenol, **1** (0.79 g, 2 mmol), was dissolved in hexane (40 mL). $Zn\{N(SiMe_3)_2\}_2$ (0.27 mL, 1 mmol) was added via syringe. The solution became cloudy upon stirring for 3 h. A colorless precipitate of **3** was isolated in *ca.* 90% yield. Small colorless crystals could be obtained from hexane, in which **3** was found to be slightly soluble; mp 254–256 °C. ^1H NMR (PhMe-d_8): δ 1.98 (s, 12H, o-Me), 2.30 (s, 6H, p-Me), 6.78 (s, 4H, m-H (Mes)), 6.63 (d, 2H, m-H (Ph)), 6.90 (t, 1H, p-H). ^{77}Se NMR ($CDCl_3$): δ −241.93 (s). IR (Nujol, ν in cm^{-1}): 1725 m, 1610 s, 1560 m, 1300 w, 1260 w, 1235 w, 1180 w, 1160 w, 1100 w, 1090 m, 1025 s, 900 m, 875 m, 850 s, 795 s, 775 m, 740 m, 580 m, 565 m, 540 m, 420 m, 345 m, 285 w.

$Zn(SeC_6H_3\text{-}2,6\text{-}Mes_2)_2(THF)$ (4). $Zn(SeC_6H_3\text{-}2,6\text{-}Mes_2)_2$, **3**, was dissolved in tetrahydrofuran (25 mL). The volume was reduced to incipient crystallization and the mixture was cooled for 24 h in the −20 °C freezer to produce **4** as colorless crystals; mp 254–256 °C (desolvation >150 °C). ^1H NMR (PhMe-d_8): δ 1.447 (m, THF), 1.98 (s, 12H, o-Me), 2.22 (s, 6H, p-Me), 3.53 (t, THF), 6.64 (d, 2H, m-H (Ph)), 6.78 (s, 4H, m-H (Mes)), 6.91 (t, 1H, p-H). ^{77}Se NMR (PhMe-d_8): δ 4.60 (s). IR (Nujol, ν in cm^{-1}): 1730 m, 1610 s, 1570 s, 1305 w, 1260 w, 1235 m, 1175 s, 1105 m, 1085 m, 1070 w, 1030 s, 975 m, 920 s, 870 s, 850 s, 800 s, 780 m, 740 s, 710 m, 670 m, 570 s, 545 m, 420 m, 345 m, 315 m, 230 m.

$Mn(SeC_6H_3\text{-}2,6\text{-}Mes_2)_2{\cdot}2CH_2Cl_2$ ($5{\cdot}2CH_2Cl_2$). The selenol, **1** (0.79 g, 2 mmol), was dissolved in hexane (40 mL), and $Mn\{N(SiMe_3)_2\}_2$ (1.7 mL of a 0.6 M solution in hexane, 1 mmol) was added via syringe. The solution became cloudy upon stirring for 3 h. A colorless precipitate of **3** was isolated in *ca.* 80% yield. Yellow crystals that were suitable for X-ray crystallography were grown from methylene chloride (7 mL): mp 315–317 °C. $\mu = 4.4\ \mu_B$ at 25 °C. ^1H NMR (PhMe-d_8): δ −10.2 (s, broad), 13.8 (s, broad), 29.2 (s, broad), 32.5 (s, broad). IR (Nujol, ν in cm^{-1}): 1715 m, 1610 m, 1565 m, 1300 w, 1260 w, 1160 m, 1090 w, 1030 s, 965 w, 885 w, 845 s, 795 s, 770 w, 735 s, 720 s, 570 m, 540 w, 425 w, 335 w. UV/vis: featureless with a slow rise toward the UV region.

$[Mn(SeMes^*)_2THF]_2{\cdot}4PhMe$ ($6{\cdot}4PhMe$). $Mn\{N(SiMe_3)_2\}_2$ (0.56 g, 2.98 mmol) was dissolved in toluene (15 mL), and the mixture was treated with a solution of 0.97 g of $HSeMes^*$ in THF (5 mL) and toluene (15 mL). The solution was allowed to stir for 12 h at room temperature, during which time a color change from pale pink to pale yellow was observed. Filtration through a Celite padded filter frit, reduction of the volume to *ca.* 10 mL under reduced pressure, and storage of the solution at *ca.* −40 °C for 16 h in the freezer afforded extremely air-sensitive colorless crystals of **6** in *ca.* 50% yield. The crystals decompose rapidly upon removal from the mother liquor to the diselenide $(SeMes^*)_2$ (authenticated by melting point and NMR studies) and a black insoluble deposit.

X-ray Crystallographic Studies

The crystals were removed from the Schlenk tube under a stream of nitrogen and immediately covered with a layer of hydrocarbon oil.

---

(19) (a) Power, P. P.; Shoner, S. C. *Angew. Chem., Int. Ed. Engl.* **1990**, *29*, 1403. (b) Bochmann, M.; Bwembya, G. C.; Grinter, R.; Lu, J.; Webb, K. J.; Hursthouse, M. B.; Mazid, M. A. *Inorg. Chem.* **1993**, *32*, 532.

(20) (a) Bonasia, P. J.; Arnold, J. *Inorg. Chem.* **1992**, *31*, 2508. (b) Seligson, J. L.; Arnold, J. *J. Am. Chem. Soc.* **1993**, *115*, 5214. (c) Bonasia, P. J.; Gindelberger, D.; Arnold, J. *Inorg. Chem.* **1993**, *32*, 5126. (d) Bonasia, P. J.; Mitchell, G. P.; Hollander, F. J.; Arnold, J. *Inorg. Chem.* **1994**, *33*, 1797.

(21) Ellison, J. J.; Ruhlandt-Senge, K.; Power, P. P. *Angew. Chem., Int. Ed. Engl.* **1994**, *33*, 1178.

(22) Ellison, J. J.; Power, P. P. *Inorg. Chem.* **1994**, *33*, 4231.

(23) (a) Ruhlandt-Senge, K.; Ellison, J. J.; Wehmschulte, R. J.; Pauer, F.; Power, P. P. *J. Am. Chem. Soc.* **1993**, *115*, 11353. (b) Du, C. F.; Hart, H.; Ng. K. D. *J. Org. Chem.* **1986**, *51*, 3162.

(24) Bürger, H.; Sawodny, W.; Wannagat, U. *J. Organomet. Chem.* **1965**, *3*, 113.

(25) Bürger, H.; Wannagat, U. *Monatsh. Chem.* **1963**, *94*, 1007.

Table 1. Abridged Summary of Data Collection Parameters for **2**−**6**[a]

	2	**3**	**4**	**5**$\cdot 2CH_2Cl_2$	**6**$\cdot$4PhMe
formula	$C_{48}H_{50}Se_2$	$C_{48}H_{50}SeZn$	$C_{52}H_{58}OSe_2Zn$	$C_{49}H_{52}Cl_2MnSe_2$	$C_{108}H_{164}Mn_2O_2Se_4$
fw	784.8	850.2	922.3	924.6	1920.1
color and habit	dichroic yellow/red cubes	colorless prisms	colorless cubes	yellow blocks	colorless needles
crystal size, mm^3	0.16 × 0.32 × 0.76	0.05 × 0.17 × 0.25	0.12 × 0.22 × 0.40	0.32 × 0.32 × 0.52	0.04 × 0.12 × 0.58
a, Å	16.144(4)	9.319(3)	10.622(4)	20.061(5)	19.000(8)
b, Å	15.123(4)	10.904(4)	10.819(5)	14.705(5)	19.626(6)
c, Å	16.155(4)	11.760(6)	22.492(6)	15.781(5)	27.687(7)
α, deg	62.60(2)	88.53(3)			
β, deg	91.86(2)	86.96(3)	85.20(3)	98.18(5)	
γ, deg	68.93(2)	60.66(2)			
V, Å^3	3942.1(17)	980.8(5)	2245.0(11)	4656(2)	10217(6)
Z	4	2	2	8	4
space group	$P2_1/n$	$P\bar{1}$	$P\bar{1}$	Pccn	$P2_1/n$
d(calc), g/cm^3	1.322	1.439	1.364	1.44	1.248
linear abs coeff, cm^{-1}	1.908	3.226	2.878	2.11	40.31
2θ range, deg	0−50	0−115.0	0−144.0	0−53	0−108.5
no. of obs reflns	4577 ($F > 4.0\sigma(F)$)	2098 ($F > 4.0\sigma(F)$)	5072 ($F > 4.0\sigma(F)$)	2859 ($F > 4.0\sigma(F)$)	4679 ($I > 3.0\sigma(I)$)
no. of variables	451	232	505	258	514
R, R_w	0.056, 0.071	0.059, 0.074	0.073, 0.106	0.063, 0.058	0.086, 0.116

[a] Data were collected at 130 K using a Siemens R3m/V diffractometer, Mo Kα (λ = 0.710 73 Å), for **2** and **5**, a Syntex P21 diffractometer, Cu Kα (λ = 1.541 78 Å) for **3** and **4**, and a Siemens P4/RA, Cu Kα (λ = 1.541 78 Å), for **6**.

A suitable crystal was selected, attached to a glass fiber, and immediately placed in a low-temperature nitrogen stream as described in ref 26.

The data for **2**, **3**, **4**, and **6** were collected at 130 K with the use of a Syntex $P2_1$ diffractometer (Cu Kα radiation, λ = 1.541 78 Å), and the data for **5** were collected at 130 K by using a Siemens R3m/V diffractometer (Mo Kα radiation, λ = 0.710 73 Å). Both diffractometers were equipped with a graphite monochromator and a locally modified Enraf-Nonius universal low-temperature device.

Crystallographic programs used for the structure solutions and refinements were those of SHELXTL-Plus installed on a MicroVax 3200 work station. Scattering factors were obtained from ref 27. An absorption correction was applied by using the method described in ref 28. Some details for the data collection and refinement, atomic coordinates, bond distances, and bond angles are available in the supplementary material. All of the structures were solved by direct methods and difference Fourier maps. The structures were refined by full-matrix least-squares procedures. All non-hydrogen atoms were refined anisotropically. Hydrogen atoms were included in the refinement at calculated positions using a riding model with C−H = 0.96 Å and U_H(iso) ~ $1.3U_C$. Some details of the crystallographic data are given in Table 1, coordinates for important atoms are given in Table 2, and selected bond distances and angles are provided in Table 3.

Results

Structural Descriptions. $(SeC_6H_3$-2,6-$Mes_2)_2$, 2. The structure of **2** (Figure 1) consists of discrete noninteracting molecules. The Se−Se−C angle is 102.5°, and the Se−Se bond length is 2.339(1) Å. The torsion angle between Se−C vectors is 128.3°.

$Zn(SeC_6H_3$-2,6-$Mes_2)_2$, 3. The structure of **3** (Figure 2) consists of monomers with no close interactions between neighboring molecules. The zinc atom lies on an inversion center in a two-coordinate environment and is bound by two selenolate ligands with a crystallographically required Se−Zn−Se angle of 180°. The Zn−Se bond length is 2.289(1) Å. The Zn−Se−C(1) angle is 106.3°. The closest interaction between the zinc center and ortho mesityl substiuents of the organic group is in excess of 3.00 Å.

$Zn(SeC_6H_3$-2,6-$Mes_2)_2$(THF), 4. The structure of **4** (Figure 3) reveals a neutral monomer with no interactions with neighboring molecules. The zinc center, which is bound to two selenolate ligands and a tetrahydofuran donor molecule, has an almost planar three-coordinate geometry. The Zn−Se(1) and Zn−Se(2) distances are 2.339(2) and 2.337(2) Å, respectively. The Zn−O(1) distance is 2.082(4) Å. The Se(1)−Zn−Se(2) angle is 150.0(1)°, and the O(1)−Zn−Se(1) and O(1)−Zn−Se(2) angles are 105.0(1)° and 104.0(1)°, respectively.

$Mn(SeC_6H_3$-2,6-$Mes_2)_2\cdot 2CH_2Cl_2$, 5$\cdot 2CH_2Cl_2$. Compound **5** (Figure 4) cocrystallizes with one molecule of methylene chloride per asymmetric unit. No interactions between the CH_2Cl_2 and the manganese are apparent. However, the CH_2Cl_2 molecules are positioned such that there are distances of 3.38 and 2.77 Å between the hydrogen atoms of this molecule and selenium and the centroid of the C(7) mesityl ring (see illustration in the Table of Contents). The manganese center, which lies on a 2-fold rotation axis, has a bent two-coordinate geometry with an Se−Mn−Se angle of 119.9(1)°. The Mn−Se bond lengths are symmetrically equivalent at 2.498(1) Å as are the Mn−Se−C(1) angles of 105.8(2)°. The closest interactions between the manganese center and ortho mesityl substituents are Mn- -C(16) (2.696 Å), Mn- -C(17) (2.716 Å), and Mn- -C(21) (2.988 Å).

$[Mn(SeMes^*)_2THF]_2\cdot$4PhMe, (6$\cdot$4PhMe). The structure of this compound is represented by the drawing in Figure 5. The basic structural motif consists of dimers formed by the association of $Mn(SeMes^*)_2$ monomeric units. Thus, there are two bridging and two terminal −SeMes* ligands. The average Mn−Se (terminal) distance is 2.466(4) Å whereas the average Mn−Se (bridging) distance is 2.60(2) Å. The average Mn−Se(t)−C angle is near 102°. The coordination of the bridging selenium centers is variable with the angular sums (Σ°) at Se(2) and Se(4) of 344 and 359.9°. The coordination spheres at the Mn centers are completed by the presence of one THF donor at each metal for which the Mn−O distances are 2.130(13) Å (Mn(1)) and 2.114(13) Å (Mn(2)). The THF's are coordinated in such a way that they have a cis-configuration with respect to the plane of the Mn_2Se_2 core. The shortest Mn- -C contacts involve C(16), C(17), and C(40) with distances of 3.091, 3.096, and 3.121 Å.

Discussion

Both the new selenol $HSeC_6H_3$-2,6-Mes_2, **1**, and the diselenide $(SeC_6H_3$-2,6-$Mes_2)_2$, **2**, can be readily synthesized in

---

(26) Hope, H. In *ACS Symposium Series No. 357*; American Chemical Society: Washington, DC, Chapter 10, p 257.

(27) *International Tables for Crystallography*; D. Reidel Publishing Co.: Boston, 1993; Vol. C.

(28) Moezzi, B. Ph.D. Dissertation, University of California, Davis, 1987.

Table 2. Atomic Coordinates ($\times 10^4$) of Important Atoms for **2**–**6**

	x	*y*	*z*
	Compound **2**		
Se(1)	7994(1)	1595(1)	5377(1)
Se(2)	7433(1)	2330(1)	4215(1)
C(1)	8798(4)	2434(4)	5803(4)
C(25)	6261(4)	2261(4)	4394(4)
	Compound **3**		
Zn(1)	0(0)	0(0)	5000(0)
Se(1)	967(1)	1351(1)	3233(1)
C(1)	2390(9)	−56(8)	2742(7)
C(2)	3468(9)	442(8)	1948(7)
C(3)	4581(9)	−511(8)	1609(7)
C(4)	4648(10)	−1946(9)	1982(8)
C(5)	3551(9)	−2392(8)	2714(7)
C(6)	2420(9)	−1488(8)	3112(7)
C(7)	1228(9)	−2047(8)	3830(7)
C(8)	1609(9)	−3142(8)	5162(7)
C(9)	546(9)	−3765(8)	5757(8)
C(10)	−872(10)	−3376(8)	5111(8)
C(11)	−1232(10)	−2305(9)	3801(8)
C(12)	−189(9)	−1657(8)	3162(8)
C(13)	3153(10)	−3635(9)	5890(8)
C(14)	−2010(11)	−4068(10)	5834(9)
C(15)	−587(10)	−570(9)	1745(8)
	Compound **4**		
Zn(1)	2619(1)	−37(1)	2504(1)
Se(1)	1637(1)	674(1)	3485(1)
Se(2)	2719(1)	452(1)	1488(1)
O(1)	4060(5)	−2200(5)	2548(2)
C(1)	2257(7)	1950(7)	3745(3)
C(25)	789(7)	1175(7)	1251(3)
	Compound **5**		
Mn	7500	2500	−123(1)
Se(1)	7178(1)	1097(1)	670(1)
C(1)	7841(3)	202(4)	394(4)
C(2)	8408(3)	434(4)	−101(4)
C(3)	8885(3)	−219(4)	−258(4)
C(4)	8820(4)	−1100(5)	35(5)
C(5)	8264(4)	−1322(4)	496(4)
C(6)	7772(3)	−690(4)	694(4)
C(16)	8509(3)	1351(4)	−477(4)
C(17)	8228(3)	1544(4)	−1269(4)
C(18)	8384(3)	2374(4)	−1662(4)
C(19)	8830(3)	2993(4)	−1316(4)
C(20)	9090(3)	2781(4)	−522(4)
C(21)	8940(3)	1984(4)	−94(4)
C(22)	7800(3)	864(4)	−1715(4)
C(23)	9000(3)	3866(4)	−1744(4)
C(24)	9230(4)	1798(5)	759(4)
C(25)	5633(4)	680(5)	2021(5)
Cl(1)	5183(1)	616(2)	1085(1)
Cl(2)	5095(1)	622(2)	2909(2)
	Compound **6**		
Se(1)	3891(1)	6818(1)	2768(1)
Se(2)	5947(1)	6405(1)	2092(1)
Se(3)	7655(1)	7871(1)	2696(1)
Se(4)	6092(1)	6613(1)	3312(1)
Mn(1)	5017(1)	6227(2)	2700(1)
Mn(2)	7024(2)	6776(2)	2720(1)
O(15)	4951(6)	5146(6)	2643(4)
O(25)	7650(6)	5881(7)	2784(5)
C(1)	3217(9)	6052(10)	2787(5)
C(101)	5914(9)	6905(8)	1444(6)
C(201)	8653(8)	7567(10)	2740(4)
C(301)	6068(10)	6672(8)	4022(6)

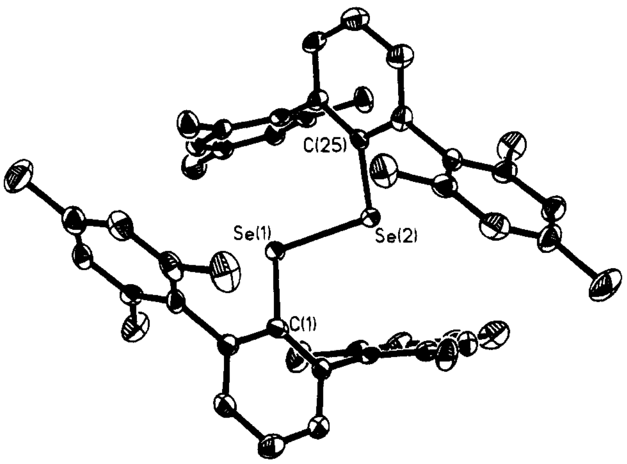

Figure 1. Computer-generated thermal ellipsoid drawing of **2**. Hydrogen atoms are omitted for clarity.

Table 3. Selected Bond Distances (Å) and Angles (deg) for **2**–**6**

		Compound **2**	
Se(1)−Se(2)	2.339(1)	Se(2)−Se(1)−C(1)	102.2(2)
Se(1)−C(1)	1.927(6)	Se(1)−Se(2)−C(25)	102.2(2)
Se(2)−C(25)	1.926(6)		
		Compound **3**	
Zn(1)−Se(1)	2.289(1)	Se(1)−Zn(1)−Se(1A)	180.0(1)
Se(1)−C(1)	1.929(9)	Zn(1)−Se(1)−C(1)	106.3(2)
Zn- -C(7)	3.002		
Zn- -C(8)	3.124		
		Compound **4**	
Zn(1)−Se(1)	2.339(2)	Se(1)−Zn(1)−Se(2)	150.9(1)
Zn(1)−Se(2)	2.337(2)	Se(1)−Zn(1)−O(1)	105.0(1)
Zn(1)−O(1)	2.082(4)	Se(2)−Zn(1)−O(1)	104.0(1)
Se(1)−C(1)	1.919(9)	Zn(1)−Se(1)−C(1)	107.7(2)
Se(2)−C(25)	1.921(7)	Zn(1)−Se(2)−C(25)	106.3(2)
		Compound **5**	
Mn−Se(1)	2.498(1)	Se(1)−Mn−Se(1a)	119.9(1)
Se(1)−C(1)	1.920(6)	Mn−Se(1)−C(1)	105.8(2)
Mn- -C(16)	2.696	C(25)−H(25a)- -Se(1)	109.5(2)
Mn- -C(17)	2.716	C(25)−H(25b)- -C(7) centroid	166.0(1.0)
Mn- -C(21)	2.988		
		Compound **6**	
Se(1)−Mn(1)	2.465(4)	Mn(1)−Se(1)−C(1)	102.5(5)
Se(2)−Mn(1)	2.632(4)	Mn(1)−Se(2)−Mn(2)	98.4(1)
Se(2)−Mn(2)	2.594(4)	Mn(1)−Se(2)−C(101)	133.4(5)
Se(3)−Mn(2)	2.467(4)	Mn(2)−Se(2)−C(101)	112.2(5)
Se(4)−Mn(2)	2.597(4)	Mn(2)−Se(3)−C(201)	101.6(6)
Se(4)−Mn(1)	2.575(4)	Mn(1)−Se(4)−Mn(2)	99.7(1)
Mn(1)−O(15)	2.130(13)	Mn(1)−Se(4)−C(301)	122.9(6)
Mn(2)−O(25)	2.114(13)	Mn(2)−Se(4)−C(301)	137.3(6)
Se(1)−C(1)	1.978(18)	Se(1)−Mn(1)−Se(2)	131.0(1)
Se(2)−C(101)	2.037(17)	Se(1)−Mn(1)−Se(4)	115.3(1)
Se(3)−C(201)	1.975(16)	Se(2)−Mn(1)−Se(4)	80.8(1)
Se(4)−C(301)	1.976(18)	Se(1)−Mn(1)−O(15)	115.6(3)
		Se(2)−Mn(1)−O(15)	97.1(4)
		Se(4)−Mn(1)−O(15)	112.0(3)
		Se(2)−Mn(2)−Se(3)	124.5(1)
		Se(2)−Mn(2)−Se(4)	81.1(1)
		Se(3)−Mn(2)−Se(4)	120.1(2)
		Se(2)−Mn(2)−O(25)	101.8(3)
		Se(3)−Mn(2)−O(25)	117.1(4)
		Se(4)−Mn(2)−O(25)	105.7(4)

moderate yields by standard synthetic routes. The ^{77}Se NMR data for **1** ($\delta = 66.7$) and **2** ($\delta = 421.5$) are well within the normal ranges as is the $J_{\mathrm{Se-H}}$ value of 61 Hz.[29] The crystal structure of **2** shows that the Se−Se distance (2.339(1) Å) is normal (cf. radius of Se = 1.17 Å)[30] and no weakening of this bond, as a result of the large substituents, is apparent. The torsion angle between Se−C vectors of 128.3° is unusually large, falling outside the normal range (74−87°) for other diselenides.[31]

---

(29) Mason, J. *Multinuclear NMR*; Plenum Press: New York, 1987; p 421.

(30) Huheey, J. E. *Inorganic Chemistry*, 3rd ed., Harper and Row: New York, 1983; p 258.

(31) Back, T. G.; Codding, P. W. *Can. J. Chem.* **1983**, *61*, 2749.

(32) Wagner, I.; du Mont, W.-W.; Pohl, S.; Saak, W. *Chem. Ber.* **1990**, *123*, 2325.

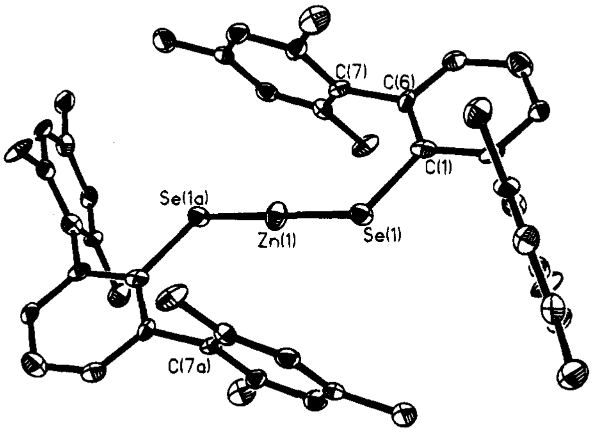

Figure 2. Computer-generated thermal ellipsoid drawing of **3**. Hydrogen atoms are omitted for clarity.

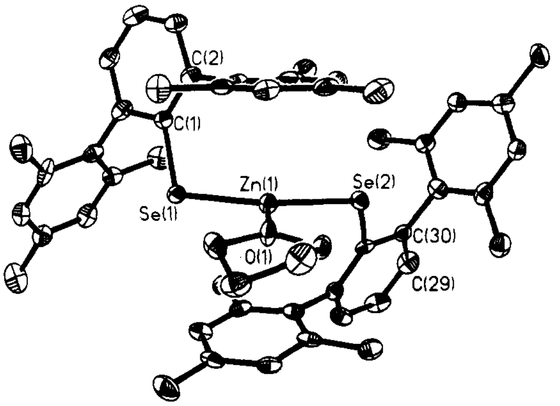

Figure 3. Computer-generated thermal ellipsoid drawing of **4**. Hydrogen atoms are omitted for clarity.

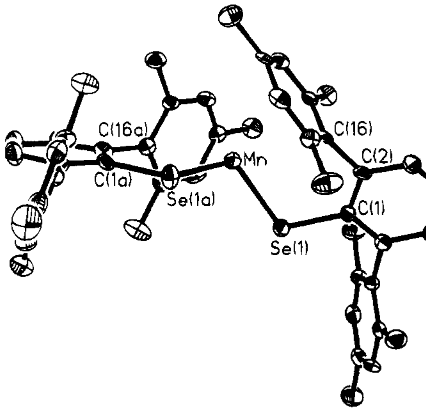

Figure 4. Computer-generated thermal ellipsoid drawing of **5**. Hydrogen atoms are omitted for clarity.

This is possibly a result of steric interactions between the large substituents.[32]

The zinc derivative **3** was synthesized in good yield by selenolysis of the amide $Zn\{N(SiMe_3)_2\}_2$ with 2 equiv of the selenol **1**. The complexed species **4** was obtained by dissolving **3** in THF and allowing the product to crystallize. The structure of this THF complex has similarities to those already reported for $Zn(SeMes^*)_2(OSC_4H_8)$[14] (**7**) and $Zn\{SeC_6H_2\text{-}2,4,6\text{-}(CF_3)_3\}_2\{HN(SiMe_3)_2\}$[15] (**8**). The Zn–Se distance observed in **4** (2.338(2) Å) is very similar to those observed in **7** (2.313(3) Å) and **8** (average 2.36 Å). A major structural difference, however, relates to the Se–Zn–Se angle which in **4** is 150.9(1)°. This value is considerably greater than the 129.0(2)° in **7** and the 133.4° in **8**. In addition, the Zn–O distance in **4**, 2.082(4) Å, is considerably longer than the Zn–O bond length observed in **7** (1.925(11) Å), although it should be mentioned that the donor in **7**, OSC_4H_8, is considerably different from THF. It is probable that the structural differences between **4** and **7**, **8** are mainly a consequence of the larger size of the $-SeC_6H_3\text{-}2,6\text{-}Mes_2$ ligand which tends to widen the Se–Zn–Se angle and weaken the coordination of other ligands in the coordination sphere.

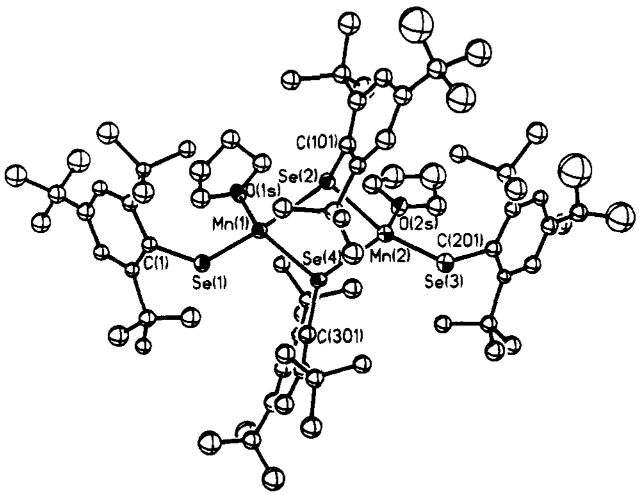

Figure 5. Computer-generated thermal ellipsoid drawing of **6**. Hydrogen atoms are omitted for clarity.

The compound $Zn(SeC_6H_3\text{-}2,6\text{-}Mes_2)_2$, **3**, and the related species $Mn(SeC_6H_3\text{-}2,6\text{-}Mes_2)_2$, **5**, are respectively the first instances of a two-coordinate zinc selenolate and an open-shell two-coordinate transition metal selenolate[33] species. The Zn–Se distance in **3**, 2.289(1) Å, is considerably shorter than those seen in **4**, **7**, and **8** which is, presumably, a consequence of the lower coordination number. The exactly linear coordination observed at zinc is something of a surprise since the corresponding thiolate derivative $Zn(SC_6H_3\text{-}2,6\text{-}Mes_2)_2$[22] (**9**) (which is not isomorphous with **3**) has a bent geometry (S–Zn–S = 151.7°) at zinc. This is opposite to what is expected on steric grounds since **3** is the sterically less encumbered molecule owing to the larger size of selenium. There is no obvious and simple explanation for the differences between the zinc thiolate and selenolate structures. However, several factors are relevant to a discussion of the setting of the geometry of two-coordinate metal compounds. For example, metal size, metal–ligand bond length, type of ligand, and the electronic properties of the metal itself are obviously of considerable importance. Thus, on average, zinc complexes would be expected to display wider angles than complexes of manganese or iron since the smaller zinc atom imposes the higher steric requirements. Longer metal–ligand bonds should also ease the steric requirements and allow greater bending at the metal. However, it appears that the most important factor in promoting bending in two-coordinate complexes is the electronic configuration of the central metals. Thus, **5** and the recently reported iron derivative $Fe(SC_6H_3\text{-}2,6\text{-}Mes_2)_2$[21] (**10**) (both with open d-shells and high-spin electron configurations) have interligand angles near 120°. It is doubtful that the possible interactions between the CH_2Cl_2 molecule and Se in the structure of **5** play any significant structural role other than one which facilitates crystallization. The Se- -H distance (3.38 Å) is rather long as is the possible interaction (2.77 Å) between H(25B) and the centroid of the

---

(33) The related homoleptic tellureolates $M\{TeSc(ScMe_3)_3\}_2$ (M = Mn or Fe) were synthesized but not purified in the following: Gindelberger, D. E.; Arnold, J. L. *Inorg. Chem.* **1993**, *32*, 5813.

C(7) ring. The latter distance is rather longer than the 2.46 Å observed in CH_2Cl_2–calixarene complexes.[34]

Significant bending has also been observed in other two-coordinate transition metal complexes.[35] The low-lying d-orbitals in these metals are only partially full and thus may interact with any available electron density, such as the π-electron clouds of the ortho substituents. The bent complexes show significantly closer M- -C interactions than those observed for linear geometry. A reasonable assumption therefore might be that a bent geometry is observed because bending allows closer M- -C interactions. However, this is not the whole story. In fact, the distance between the metal and the ortho substituents in aryl chalcogenolate complexes is primarily a function of the torsion angle between the M–E–C(ipso) (E = S, Se) plane and the plane of the C(ipso) ring—and not the amount of bending at the metal. The closest M- -C approaches are observed for the smaller torsion angles. This correlation is observed in **3** (torsion angle 19.7°), **5** (torsion angle 5.7°), and **10** (torsion angles 4.0° for the ring with the closest M••C interactions). Consideration of the geometry of the ortho-substituted aryl groups employed here and the relatively narrow M–E–C (E = S, Se) angles near 105° suggests that a linear geometry at the metal plus a zero torsion angle (as defined above) would lead to undue steric congestion. In the absence of any significant interaction between an ortho substituent and the metal, the torsion angle increases to ease steric crowding (although the planes of the two aromatic rings attached to selenium remain parallel), and this is what is observed in the case of the zinc derivative **3**. Where there is a significant interaction between the ortho substituent and the metal as in **5** or **10**, a small torsion angle is required for the closest M- -C approach, which is again sterically incompatible with a linear geometry. Molecules can avoid this steric congestion and preserve the close M- -C interaction by bending. The preservation of the close M- -C interactions in the bent molecule results in an almost perpendicular orientation of the planes of the aromatic rings attached to selenium in order to minimize the steric congestion. The arguments made above may be summarized by saying that currently known open-shell two-coordinate compounds that have ligands substituted by aromatic groups adopt a bent configuration for steric reasons in order to preserve interactions between the metal d-orbitals and the electron-rich aromatic groups in these ligands.

In addition to these intramolecular considerations, there is the possibility of competitive intermolecular interactions involving the aromatic rings of the substituents which is maximized when the rings are aligned parallel to each other. This may be the key factor in determining the linear coordination of **3**, where it can be seen (Figure 6) that this geometry allows parallel orientation of the mesityl substituents. This does not occur in the manganese analogue **5**.

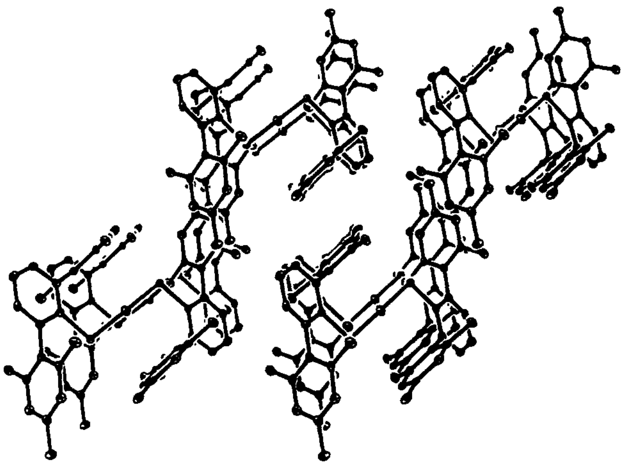

Figure 6. View of the intermolecular packing of **3** showing the parallel orientation of the mesityl rings. Hydrogen atoms are omitted for clarity.

The structure of the dimeric compound **6** underlines the steric and electronic differences between the –Mes* and $-C_6H_3$-2,6-Mes_2 substituents. The dimeric structure of **6** is preserved even in the presence of THF donor ligands. (It has not yet proved possible to grow crystals of a THF complex of **3** suitable for X-ray crystallography although such a complex is presumably monomeric.) The metric features of **6** demonstrate that the bridging Mn–Se distances are significantly (ca. 0.15 Å) longer than the terminal Mn–Se bonds. Oddly, the terminal Mn–Se distances, average 2.466(4) Å, are marginally shorter than the Mn–Se bond lengths in the nominally two-coordinate complex **5**. This is in agreement with the relatively long Fe–S distances in $Fe(SC_6H_3\text{-}2,6\text{-}Mes_2)_2$[21] which are similar to those in some four-coordinate Fe–S species.[36]

Acknowledgment. We thank the donors of the Petroleum Research Fund, administered by the American Chemical Society, and the National Science Foundation for financial support.

Supplementary Material Available: Tables giving full details of the crystal data and crystallographic data collections, atom coordinates, bond distances, bond angles, and thermal parameters for **2–6** (58 pages). Ordering information is given on any current masthead page.

IC941001T

---

(34) Atwood, J. L.; Bott, S. G.; Jones, C.; Raston, C. L. *J. Chem. Soc., Chem. Commun.* **1992**, 1349.

(35) Power, P. P. *Comments Inorg. Chem.* **1989**, *8*, 177.

(36) (a) Koch S. A.; Maelia, L. E.; Millar, M. *J. Am. Chem. Soc.* **1983**, *105*, 5944. (b) Hagen, K. S.; Holm, R. H. *Inorg. Chem.* **1984**, *23*, 418.